2096–2110 *Nucleic Acids Research, 2022, Vol. 50, No. 4* *Published online 12 February 2022*
https://doi.org/10.1093/nar/gkac071

Physical ARTEMIS:DNA-PKcs interaction is necessary for V(D)J recombination

Doris Niewolik [1,*,#] and Klaus Schwarz[1,2,#]

[1]Institute for Transfusion Medicine, University of Ulm, Ulm 89081, Germany and [2]Institute for Clinical Transfusion Medicine and Immunogenetics Ulm, German Red Cross Blood Service Baden-Wuerttemberg-Hessen, Ulm 89081, Germany

Received August 09, 2021; Revised January 12, 2022; Editorial Decision January 19, 2022; Accepted January 25, 2022

ABSTRACT

The nuclease ARTEMIS and the DNA-dependent protein kinase catalytic subunit (DNA-PKcs) are involved in the repair of physiological and pathogenic DNA double strand breaks. Both proteins are indispensable for the hairpin-opening activity in V(D)J recombination and therefore essential for the adaptive immune response. ARTEMIS and DNA-PKcs interact, however experimental evidence for *in vivo* significance is missing. We demonstrate that mutations abolishing this protein-protein interaction affect nuclease function. In DNA-PKcs, mutation L3062R impairs the physical interaction with ARTEMIS and was previously identified as pathogenic variant, resulting in radiosensitive severe combined immunodeficiency. In ARTEMIS, specific mutations in two conserved regions affect interaction with DNA-PKcs. In combination they impair V(D)J recombination activity, independent of ARTEMIS autoinhibitory self-interaction between the ARTEMIS C-terminus and the N-terminal nuclease domain. We describe small fragments from both proteins, capable of interaction with the corresponding full-length partner proteins: In DNA-PKcs 42 amino acids out of FAT region 2 (PKcs3041-3082) can mediate interaction with ARTEMIS. In the nuclease we have defined 26 amino acids (ARM378-403) as minimal DNA-PKcs interacting fragment. The exact mapping of the ARTEMIS:DNA-PKcs interaction may pave the way for the design of specific inhibitors targeting the repair of DNA double strand breaks.

INTRODUCTION

In eukaryotic cells non-homologous end-joining (NHEJ) is a pathway for the repair of DNA double strand breaks (DSB), which are a major threat to genomic integrity (1,2). NHEJ also is part of the V(D)J recombination process, an essential step during lymphocyte development (3). Thereby sub-genomic elements, derived from the variable (V), diversity (D) and joining (J) regions of the immunoglobulin and T cell receptor loci, are recombined. In a first step, the lymphocyte-specific Recombination Activating Gene 1 and 2 (RAG1/2) proteins cut the DNA sequence-specifically at the recombination signal sequences (RSS) and produce hairpins at the DNA ends of the coding sequences. These physiological DSB are subsequently repaired by NHEJ, with its error prone nature contributing to the diversity of the adaptive immune system. Many different proteins take part in NHEJ, and three stages are distinguished (4–6). First, the KU70/80 heterodimer detects the DSB, recruits the DNA-dependent protein kinase catalytic subunit (DNA-PKcs) and together they tether and protect the DNA ends of the DSB. Next, nucleases and polymerases are recruited and participate in the processing of the DNA ends. The nuclease ARTEMIS is one of these enzymes and during V(D)J recombination it is essential for opening the hairpin-sealed DNA intermediates (7). The final step in NHEJ is the ligation of the processed DNA ends, conducted by DNA Ligase 4, XRCC4 and XLF. The NHEJ components associate in a multiprotein complex, containing both enzymatically active proteins (e.g. DNA-PKcs, ARTEMIS, DNA Ligase 4) and proteins functioning primarily as scaffolds (KU70/80, XRCC4/XLF) (8). It can be envisaged that specific interactions between individual proteins regulate the functional steps of NHEJ.

DNA-PKcs is a member of the family of phosphatidylinositol 3-kinase-related kinases (PIKKs), which include other serine/threonine protein kinases involved in DNA repair: Ataxia telangiectasia mutated (ATM) and ataxia-telangiectasia and Rad3-related (ATR). In all PIKKs the conserved kinase domain is located near the C-terminus, and it is surrounded by regulatory domains, such as the FAT (FRAP, ATM, TRRAP), PRD (PIKK regulatory domain) and FATC (FAT C-terminal) domains (9). DNA-PKcs and the KU70/80 heterodimer assemble at the ends of DSB (10) and form the DNA-PK holoenzyme. This association in-

*To whom correspondence should be addressed. Tel: +49 731 150 6759; Fax: +49 731 150 645; Email: doris.niewolik@uni-ulm.de
#Authors are listed in alphabetical order.

duces the kinase activity and results in autophosphorylation of DNA-PKcs (11,12).

ARTEMIS belongs to a superfamily of nucleases characterized by conserved metallo-β-lactamase and β-CASP (CPSF, ARTEMIS, SNM1, PSO2) domains (13). ARTEMIS acts on DNA substrates, specifically it recognizes single to double strand transitions (14,15). The nuclease domain resides in the N-terminal half of the protein (16,17) and ARTEMIS endonucleolytic activity, in particular the hairpin opening, is DNA-PKcs dependent (7,18). Self-interaction between the N- and C-terminal halves of ARTEMIS mediates autoinhibition of the nuclease (19). The ARTEMIS C-terminus is phosphorylated by DNA-PKcs *in vitro* (20–22) and a role of DNA-PKcs in the relief of autoinhibition is hypothesised (18,20). While there is no experimental evidence that DNA-PKcs mediated phosphorylation of ARTEMIS is of relevance *in vivo* (22), autophosphorylation of DNA-PKcs plays an important role in regulating its kinase activity (23) as well as ARTEMIS endonucleolytic activities (7,22,24).

Loss of function of most of the NHEJ factors results in radiosensitive severe combined immunodeficiency (RS-SCID, reviewed in (25)). Since the first description in 2001 (26), a defect in ARTEMIS as cause of the RS-SCID phenotype has been found in about 10% of the B^- T^- SCID patients. Most of these have either gross deletions or point mutations in the *DCLRE1C* gene, affecting the nuclease domain in the N-terminal half of the ARTEMIS protein (27). Up to now only few RS-SCID patients have been described with pathogenic variants in the *PRKDC* gene, encoding DNA-PKcs. In the first patient mutation L3062R resulted in increased numbers of P-nucleotides in the residual lymphocyte population, also observed in RS-SCID with pathogenic variants in *DCLRE1C* (28), pointing to a failure in ARTEMIS activation as cause of the immunodeficiency (29). To our knowledge all but one (30) of the additional patients described with a defect in *PRKDC,* have amino acid exchange L3062R (31,32).

ARTEMIS and DNA-PKcs interact and during V(D)J recombination both proteins together constitute the hairpin-opening activity (7). While *in vitro* nuclease assays show a DNA-PKcs dependence of ARTEMIS hairpin opening, experimental evidence for the functional significance of the ARTEMIS:DNA-PKcs interaction *in vivo* has not been put forward yet. Here we present evidence, that the interaction between ARTEMIS and DNA-PKcs is impaired by the pathogenic variant L3062R in DNA-PKcs, suggesting that this may be related to the RS-SCID phenotype. We describe a small fragment out of the FAT region in DNA-PKcs, encompassing L3062, capable of association with ARTEMIS. In ARTEMIS we identify two conserved regions that together make up the DNA-PKcs interaction domain. The combination of amino acid exchanges in both regions in full-length ARTEMIS significantly impairs V(D)J recombination activity in a newly established HCT116 *DCLRE1C*–/– knock out cell line. Thus, for the first-time evidence is provided that specific point mutations in ARTEMIS and DNA-PKcs impair both protein-protein interaction and V(D)J recombination *in vivo*.

MATERIALS AND METHODS

Reagents

The following antibodies were used for immunoprecipitations and western blotting: anti-Myc tag (Life Technologies Inc., # 46-1155 and Roche Diagnostics GmbH, # 11667203001), anti-V5 (Life Technologies Inc., # 46-1157), anti-Xpress (Life Technologies Inc., # 46-0528), anti-beta-Actin (ACTB, ab8227, Abcam), anti-DNA–PKcs (ab69527, Abcam and sc390849, Santa Cruz Biotechnology, Inc.), anti-KU70 (E5, sc-17789 and M19, sc-1487, Santa Cruz Biotechnology, Inc.), anti-Ku86 (B1, sc-5280 and C-20, sc-1484, Santa Cruz Biotechnology, Inc.), anti-ARTEMIS (Cell Signaling Technology # D708V, Biolegend # 691602). Secondary HRP-conjugated antibodies were from Bio-Rad (goat-anti-mouse IgG-HRP # 170–6516, goat-anti-rabbit IgG-HRP # 170–6515), Santa Cruz (donkey-anti-goat IgG, sc-2033) and from Rockland (Mouse TrueBlot Ultra, # 18-8817-33). Chemiluminescent substrates were from ThermoFisher Scientific (SuperSignal™ West Pico PLUS # 34579 and Femto Maximum Sensitivity Substrate, # 34095). In V(D)J recombination assays Biotin-anti-H-$2K^k$ (BD Biosciences, # 553591) antibody was used. Transfections were performed with Amaxa™ Cell line Nucleofector Kit T, Lonza (CHO derived cell lines), Amaxa™ Cell line Nucleofector Kit V, Lonza (HCT116 derived cell lines).

Biological resources

CHO V3 + YFP/PKcs, wildtype or mut (delG2113/L3062R) kindly were provided by M. van der Burg/D. van Gent/D. Chen and are described in (29). CHO-V3, CHO-V3 YFP/PKcs (WT and mut) and CHO V3-R5 cells were cultured in IMDM supplemented with 10% FCS. CHO V3-R5 and CHO-V3 YFP/PKcs were cultured in the presence of puromycin (4 μg/ml) and G418 (700 μg/ml), respectively. HEK293T cells were cultured in DMEM supplemented with 10% FCS and transfected using calcium phosphate precipitation method. HCT116 (Horizon, Cambridge) and HCT116 *DCLRE1C*–/– cells were cultured in RPMI medium, supplemented with 10%.

Generation of HCT116 DCLRE1C-/- knockout cell-line

The human ARTEMIS-knockout HCT116 cell line (HCT116 *DCLRE1C*–/–) was established using CRISPR/Cas9-mediated genome editing. Target sequences for CRISPR interference were designed using IDT Design custom gRNA software (https://eu.idtdna.com/site/order/designtool/index/CRISPR_CUSTOM). The target sequences are located in the 5`UTR and in intron 1, resulting in deletion of exon 1. CRISPR-Cas9 crRNA and the corresponding tracer RNA were obtained from Integrated DNA Technologies, BVBA, Leuven, Belgium and are specified in Supplemental Table S5. Ribonucleoprotein (RNP) complex was assembled *in vitro* by incubating CRISPR-Cas9 crRNAs and Cas 9 protein (kindly provided by S. Radecke). HCT116 parental cells (Horizon, Cambridge, UK) were subsequently transfected with the RNP, using nucleofection (Amaxa™ Cell line Nucleofector Kit T, Lonza). After 24 h single cells were seeded in 96-well

plates and incubated for 21 days, using RPMI medium supplemented with 10% FCS and antibiotics. Clones were subsequently screened by PCR and Sanger sequencing. Two different anti-ARTEMIS antibodies, directed against a region around P367 (Cell Signaling Technology # D708V) and against the C-terminal region (Biolegend # 691602), were used in expression analyses; no ARTEMIS protein was detected.

Protein expression constructs

Human wildtype (ART-WT) and mutant (ARM) ARTEMIS expression plasmids were cloned via KpnI/NotI into pcDNA6/myc-His, pcDNA6V5-His or pcDNA4His/Max vectors (Invitrogen, Breda, Netherlands). The latter constructs in addition contained at the C-terminus a Myc Fusion tag, derived from pcDNA6/myc-His. Specific amino acid exchanges were introduced using either the QuikChange Site-Directed Mutagenesis Kit (Agilent) or the NEBuilder™ HiFi DNA assembly cloning kit (New England Biolabs). Forward and reverse primers used for amplification of deletion mutants and for mutagenesis are specified in Supplemental Tables S3 and S4, respectively. The nomenclature refers to the amino acids included in the respective ARTEMIS mutant proteins and specific amino acid exchanges, see (19) for details. Human DNA-PKcs fragments were cloned via KpnI/NotI into pcDNA4His/Max and in addition contained at the C-terminus a Myc Fusion tag, derived from pcDNA6/myc-His. The amino acid exchange L3062R was introduced via the QuikChange Site-Directed Mutagenesis Kit (Agilent). Forward and reverse primers used for amplification of deletion mutants and for mutagenesis are specified in Supplemental Tables S3 and S4, respectively. The nomenclature refers to the amino acids included in the respective DNA-PKcs fragment.

Immunoprecipitation assay and immunoblotting

The immunoprecipitation assay was performed essentially as described (7,18,19) with the following modifications. Prior to immunoprecipitation with anti-Myc antibody, a preclearing step with protein G Sepharose was performed. Experiments depicted in Figure 4, Supplementary Figures S2–S4 were performed with lysis buffer containing 0.01% NP40, in Figure 6B with buffer containing 100 mM KCl and 0.1% NP40. To determine DNA-independence of protein-protein interactions, precleared lysates were incubated 30 min on ice with or without ethidium bromide (final concentration 200 μg/ml), followed by 5 min centrifugation. The supernatant was used in standard immunoprecipitation assay, in the presence or absence of ethidium bromide (200 μg/ml). Cell lysis for protein expression analysis was performed with buffer containing 50 mM Tris–HCl pH 8, 62.5 mM EDTA, 1% Nonidet 40 (NP40), 0.4% sodiumdeoxycholate.

V(D)J recombination assay

The cellular V(D)J recombination assay and FACS analyses of transfected HCT116 *DCLRE1C*–/– cells were essentially carried out as described (17), with the following modifications: in the V(D)J recombination substrate vector the inverted EGFP ORF was under the control of the EF1a promoter. Transfections in the HCT116 *DCLRE1C*–/– cells were performed with 1.6 μg pcWTRAG1, 1.2 μg pcWTRAG2, 4 μg Substrate vector 11/19H2K^{K} and varying amounts of ARTEMIS expression vector (pcDNA6ART-WT/myc, pcDNA6ARM/myc). The total amount of transfected DNA content was kept constant, using vector DNA without insert. After 48 h, cells were harvested and analysed by FACS. Cells were stained with biotin-labelled anti-mouse H-2K^{K} antibody, followed by incubation with Allophycocyanin (APC) conjugated Streptavidin (Biolegend, # 405207). Statistical evaluations of the results were performed using IBM SPSS statistics version 27.

RESULTS

The pathogenic variant L3062R in DNA-PKcs impairs its interaction with ARTEMIS

Amino acid exchange L3062R in DNA-PKcs has no impact on protein stability, DNA end-binding and kinase activity (29). The phenotypical similarity to RS-SCID patients with a defect in ARTEMIS indicated that variant L3062R in DNA-PKcs caused insufficient activation of this nuclease. Co-localization of ARTEMIS and mutant DNA–PKcs at sites of laser-induced DSB led to the conclusion that the interaction between DNA-PKcs and ARTEMIS is not affected by L3062R. In order to reassess this issue, we performed co-immunoprecipitation experiments to evaluate the abilities of wildtype and mutant DNA-PKcs to physically interact with ARTEMIS.

We analysed the ARTEMIS:DNA-PKcs interaction in two CHO cell lines, which express human DNA-PKcs with either wildtype sequence (CHO/PKcs WT) or harbouring the sequence variants found in the RS-SCID patient (ΔG2113 and L3062R, CHO/PKcs mut) (29). After transient expression of Myc-tagged ARTEMIS proteins, these were immunoprecipitated out of the cell lysates using anti-Myc antibody and subsequently analysed in western blotting experiments. In order to evaluate quantitative differences in the ARTEMIS interaction with wildtype or mutant DNA-PKcs protein, we performed a titration of the immunoprecipitates. The results are depicted in Figure 1, showing DNA-PKcs co-immunoprecipitations by ARTEMIS (ART-WT, lanes 1–8) and KU70/80 as control (lanes 9–14). In the case of ARTEMIS, comparable amounts of IP product and DNA-PKcs input result in 5 to 10-fold reduced co-immunoprecipitation of mutant versus wildtype DNA-PKcs (Figure 1, compare lanes 1–4 with lanes 6 and 7). There is no difference between wildtype and mutant DNA-PKcs with respect to co-immunoprecipitation by the KU70/KU80 heterodimer (Figure 1, compare lanes 9–11 to 12–14). The interaction between ARTEMIS and DNA-PKcs is DNA-independent, since it is not affected by the presence of ethidium bromide, a DNA intercalating agent which distorts the double helix (Supplementary Figure S1, lanes 1–3). As expected, the association of the KU proteins with DNA-PKcs is DNA-dependent (Supplementary Figure S1, lanes 4–6). Together these *in vitro* co-immunoprecipitation experiments establish

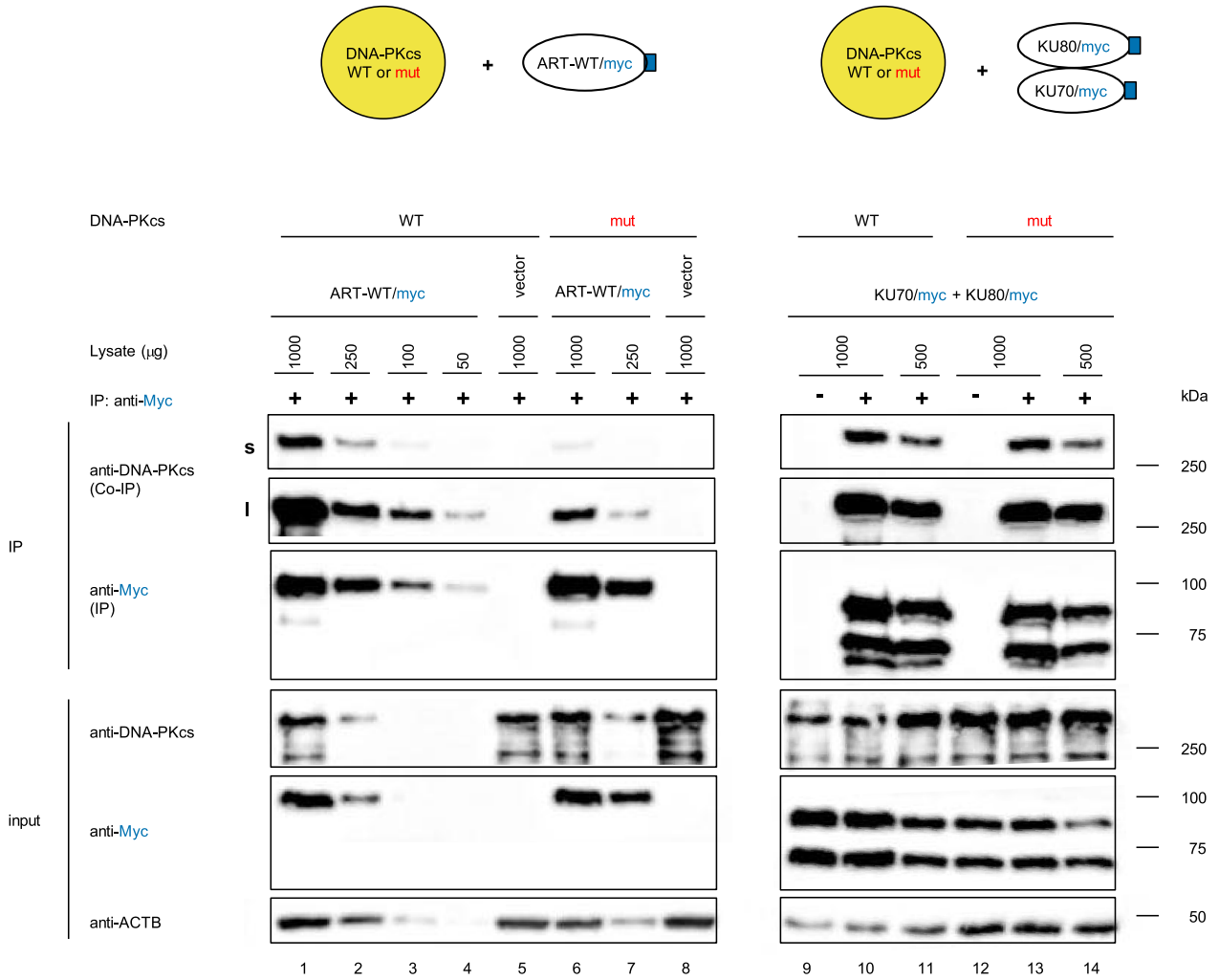

Figure 1. Pathogenic variant L3062R in DNA-PKcs impairs its interaction with ARTEMIS. ARTEMIS:DNA-PKcs interaction was analysed in two different CHO V3 derived cell lines, which stably express human YFP-tagged DNA-PKcs of either wildtype (WT) or mutant (mut; ΔG2113 + L3062R) sequence. Cells were transiently transfected with Myc-tagged ARTEMIS (ART-WT/myc) or KU70 and KU80 (KU70/myc + KU80/myc) expressing plasmids or with vector without insert (vector). The different interaction partners are represented graphically at the top, indicating the Myc Tag as blue rectangle (not to scale). Myc-tagged proteins were immunoprecipitated (IP) from cell lysates with anti-Myc antibody. In the case of ART-WT/myc (lanes 1–8) different amounts of the immunoprecipitates and the corresponding input lysates were separated in SDS-PAGE as indicated above each lane. Lanes 11 and 14 contained a 1:1 mix of cell lysates of transfections with KU70/KU80 and empty vector, in order to visualize the approximately 2-fold-reduced levels of KU70/KU80 in the cell line expressing mutant (mut) as compared to wildtype DNA-PKcs (WT) (lanes 12–14 and lanes 9–11, respectively). Western blotting was performed and co-immunoprecipitation (Co-IP) of human YFP/DNA-Pkcs was compared to input, using anti-DNA-PKcs antibody. Short (s, 30 s) and long (l, 5 min) exposures are shown for the co-immunoprecipitates. IP products were detected using anti-Myc antibody. The positions of protein standards are given at the right in kDa. An anti-β-actin (ACTB) antibody was used as loading control in input lanes. Co-immunoprecipitations were analysed in three independent experiments, a representative experiment is shown.

that patient variant L3062R in DNA-PKcs specifically impairs its interaction with the nuclease ARTEMIS. The fact that mutant DNA-PKcs assembled at sites of laser-induced DSB (29) suggests that other regions in the kinase may contribute to ARTEMIS binding in living cells and that L3062R possibly also affects additional aspects of DNA-PKcs function.

A fragment out of FR2 in DNA-PKcs can interact with ARTEMIS

Based on the above findings we wanted to determine the ARTEMIS interaction domain in DNA-PKcs. The pathogenic variant L3062R lies in the conserved FAT domain, which consists of five supersecondary structures (FR1-FR5) (33,34), with L3062 located within FR2 (Figure 2A). ATM and ATR are related PIKKS, which also phosphorylate ARTEMIS (35–38). Comparing the sequence surrounding L3062 in DNA-PKcs with the corresponding regions in ATM and ATR, little conservation is observed (Figure 2B). Potential orthologs of DNA-PKcs have been identified not only in vertebrates, but also in invertebrates, fungi, plants and protists, based on DNA sequence (39). Functional distinction from other PIKK family members has yet to be demonstrated. The region around L3062 is highly conserved in vertebrates, in representatives of other

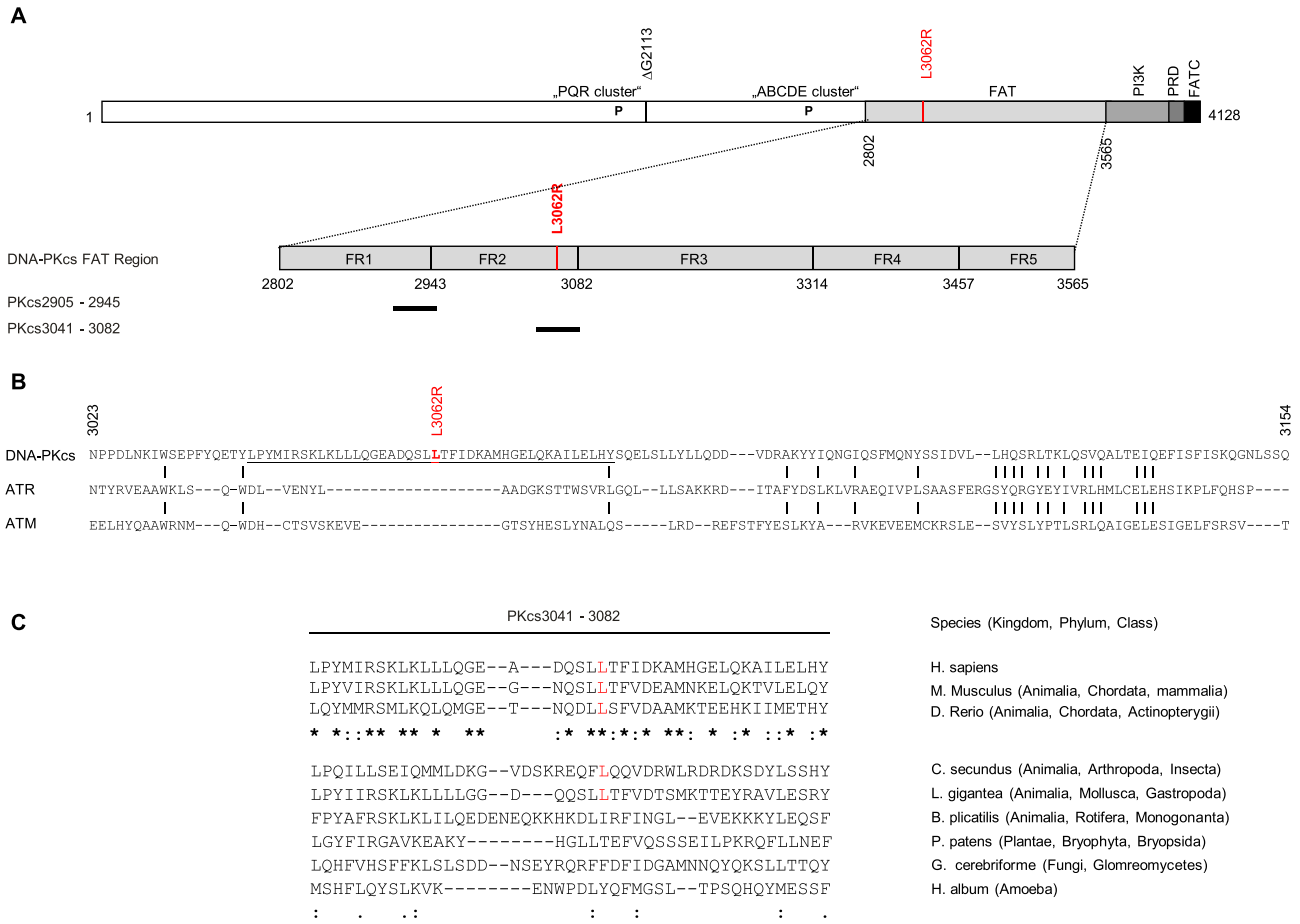

Figure 2. Schematic presentation of DNA-PKcs. (**A**) Schematic of DNA-PKcs with differently shaded domains: HEAT (white), FAT (light grey), kinase (medium grey), PRD (dark grey) and FATC (black). The variants described in the first RS-SCID patient are indicated, also autophosphorylation clusters (P). Below, there is a blow up of the FAT region, with amino acid positions corresponding to the super-secondary structures FAT region (FR) 1–5 according to (33). Horizontal lines underneath the FAT domain denote the DNA-PKcs fragments analysed in this study, specified by name on the left, defining amino acids (aa) encompassed. (**B**) Sequence alignment of parts of the FAT domains of human DNA-PKcs (aa 3023–4054), ATR (aa 1871–1972) and ATM (aa 3002–4000) using CDD homologene (60), conserved amino acids are indicated by vertical lines. The underlined sequence in DNA-PKcs corresponds to fragment PKcs3041-3082. The pathogenic variant L3062R is highlighted in red. (**C**) Sequence alignment of region PKcs3041-3082 in different species as specified. Top, sequences of three chordata, below in addition of selected species from diverse phyla (see (39) for a detailed analysis). Asterisks, colons and periods indicate fully conserved, strongly and weakly similar residues, respectively (Clustal Omega, (61)).

phyla, the leucine at position 3061 but not at 3062 is conserved (Figure 2C). We constructed expression vectors containing a fragment spanning amino acids 3041–3082 out of the FR2 in DNA-PKcs with either wildtype sequence (PKcs3041-3082) or patient variant L3062R (PKcs3041-3082 + L3062R) . As a control, we chose a fragment out of FR1, denoted PKcs2904-2945. DNA-PKcs fragments contained N-terminal Xpress and C-terminal Myc tags. Interaction with V5-tagged ARTEMIS proteins was analysed in CHO V3 cells, which are devoid of endogenous DNA-PKcs (40,41). Experiments in the CHO V3 derived cell line CHO V3-R5, which stably expresses Myc-tagged human DNA-PKcs (18) were conducted to assess interaction between ARTEMIS and full-length DNA-PKcs in a comparable experimental setting. After transient transfection, Myc-tagged full-length DNA-PKcs or DNA-PKcs fragments were immunoprecipitated from cell lysates with anti-Myc antibody. After SDS-PAGE and western blotting, binding of ARTEMIS proteins was evaluated by comparing input and immunoprecipitates using anti-V5 antibody (Figure 3).

Figure 3A shows a schematic of the different ARTEMIS proteins analysed in the co-immunoprecipitation experiments. Like full-length DNA-PKcs (Figure 3D), fragment PKcs3041-3082 interacts with ART-WT (Figure 3B) and with the C-terminal ARTEMIS fragment ARM308-692 (Figure 3C). Strikingly, the amino acid exchange L3062R in PKcs3041-3082 does not affect binding (compare lanes 2 and 3 in Figure 3B and C). The fragment derived from FR1 (PKcs2904-2945) does not interact with ARTEMIS (lane 1 in Figure 3B and C). Overexpression of ARM308-692 in CHO V3 cells results in three bands (c–e in Figure 3C, lanes 5–8), with (d) and (e) corresponding to the use of internal translational start sites at methionines in positions 348 and 418 (M348 and M418 in Figure 3A). In CHO V3 cells bands (c) and (d) are more prominent than (e) (Figure 3C, lanes 5–8), while in CHO V3-R5 cells ARM348-692 (d) is the dominant translation product (Figure 3D, lane 6). Significantly,

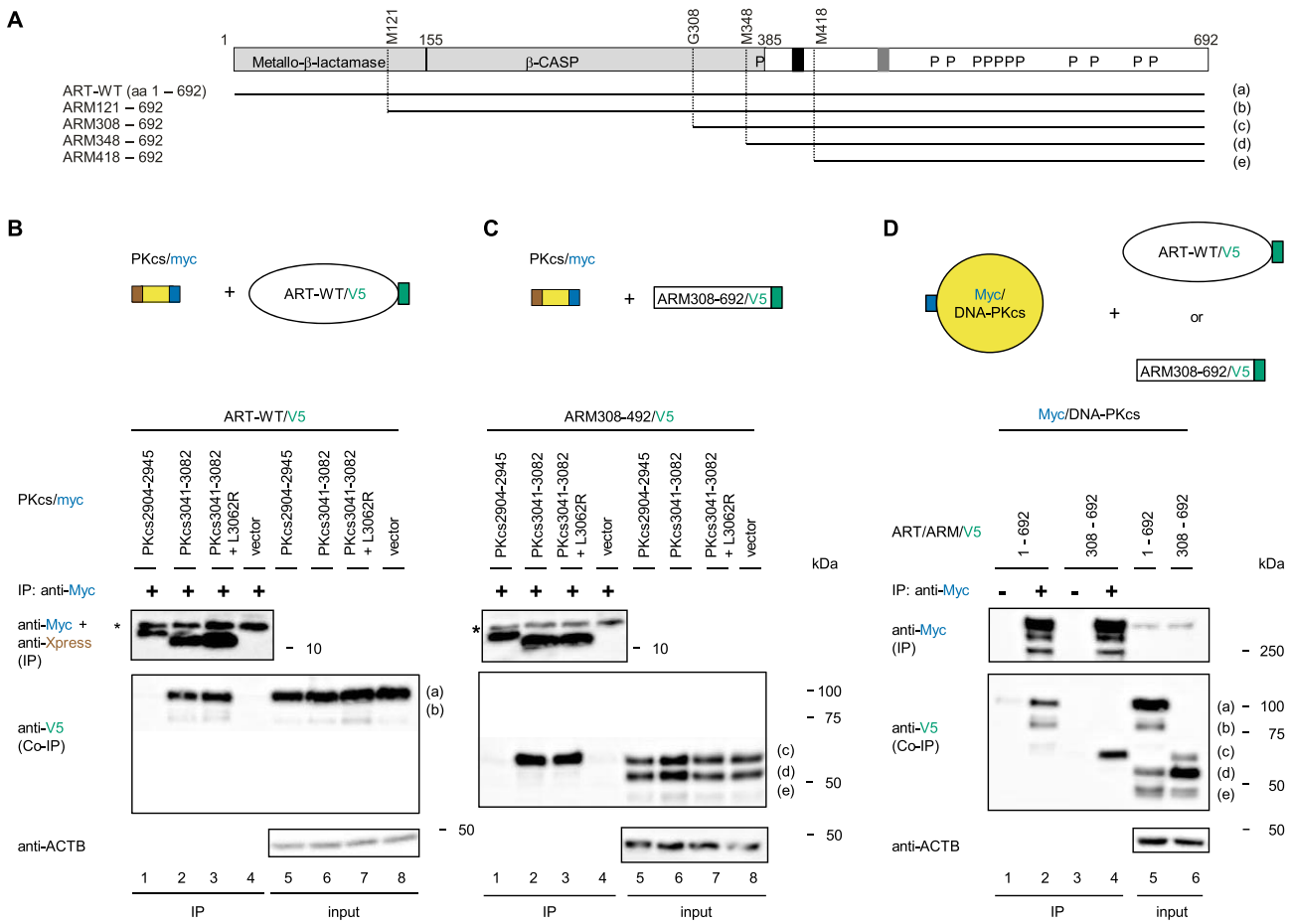

Figure 3. DNA-PKcs fragment PKcs3041-3082 interacts with ARTEMIS. (**A**) Schematic of ARTEMIS, indicating the N-terminal nuclease domain (light grey), composed of the metallo-β-lactamase and β-CASP domains, the DNA-PKcs interaction region (black) and the autoinhibitory domain (dark grey). Numbers refer to amino acid positions. P indicates *in vitro* DNA-PKcs phosphorylation sites (20–22). Methionines used as internal start sites of translation are indicated (M121, M348, M418). Below, ARTEMIS fragments are represented as black lines and specified by name on the left, defining the amino acids encompassed. On the right, small letters in brackets (a-e) refer to the corresponding bands in the western blot experiments. (**B** and **C**) Co-immunoprecipitation experiments in DNA-PKcs deficient CHO V3 cells. IP products were DNA-PKcs fragments out of FR1 (PKcs2904-2945) and FR2 (PKcs3041-3082) or vector without insert (vector) as specified above each lane. The DNA-PKcs fragments contained an N-terminal Xpress and a C-terminal Myc-tag. The vector control results in an expressed fragment, containing in frame the Xpress- and Myc-tags, which together correspond to a theoretical MW of 7 kDa. Corresponding expression plasmids were transfected in combination with plasmids for C-terminally V5-tagged ARTEMIS proteins as binding partners, with either wildtype sequence (ART-WT) in (B) or with an N-terminal deletion mutant (ARM308-692) in (C). DNA-PKcs fragments were immunoprecipitated (IP) from cell lysates with anti-Myc antibody; input lysates and 50% of the IP samples were separated in 8% SDS-PAGE for detection of the co-immunoprecipitates (Co-IP). The other 50% of the IP samples were separated in 15% SDS-PAGE. After western blotting Co-IP and IP products were detected using anti-V5 and anti-Myc plus anti-Xpress antibodies, respectively. * indicates a non-specific band, derived from the light chain of the anti-Myc antibody used for immunoprecipitation. (**D**) CHO V3-R5 cells, stably expressing a Myc-tagged human DNA–PKcs, were transiently transfected with V5-tagged ARTEMIS-expressing plasmids. Myc-tagged DNA-PKcs was immunoprecipitated (IP) from cell lysates with anti-Myc antibody; IPs and input lysates were separated in SDS-PAGE, and western blotting was performed. Co-IP of the V5-tagged proteins was compared with input, using anti-V5 antibody. IP products were identified using anti-Myc antibody. (B–D) Interacting full-length proteins (ellipses) and protein fragments (rectangles) are represented graphically at the top (not to scale). Immunological tags of IP products (Myc) and Co-IP products (V5) are indicated in blue and green, respectively. Brown rectangles correspond to N-terminal Max epitopes. The positions of protein standards are given at the right in kDa. Small letters in brackets denote the different ARTEMIS fragments as defined in (A). Anti-β-actin (ACTB) antibody was used as loading control in input lanes. Two independent co-immunoprecipitation experiments were performed, and comparable results obtained.

in both cell lines we observe co-immunoprecipitation of the upper band only (Figure 3C, lanes 2 and 3 and Figure 3D, lane 4), corresponding to ARM308-692 (c). Both full-length DNA-PKcs and PKcs3041-3082 do not co-precipitate the lower band (d, ARM348-692), although this fragment includes the previously described essential amino acids 398–403 (Figure 3A). Overexpression of ART-WT in CHO V3-R5 cells, also shows translational starts at internal methionines M348 (d) and M414 (e) and in addition at M121 (b). Again, co-immunoprecipitation is not observed for fragments (d) and (e) (Figure 3D lanes 2 and 5).

The results presented in Figure 3 show that a DNA-PKcs fragment containing 42 amino acids of FR2 (PKcs3041-3082) can interact with ARTEMIS. Both full-length DNA-PKcs and fragment PKcs3041-3082 require amino acids 308–347 in ARTEMIS for interaction. However, while the pathogenic variant L3062R in full-length DNA-PKcs impairs its interaction with ARTEMIS (Figure 1), it does not

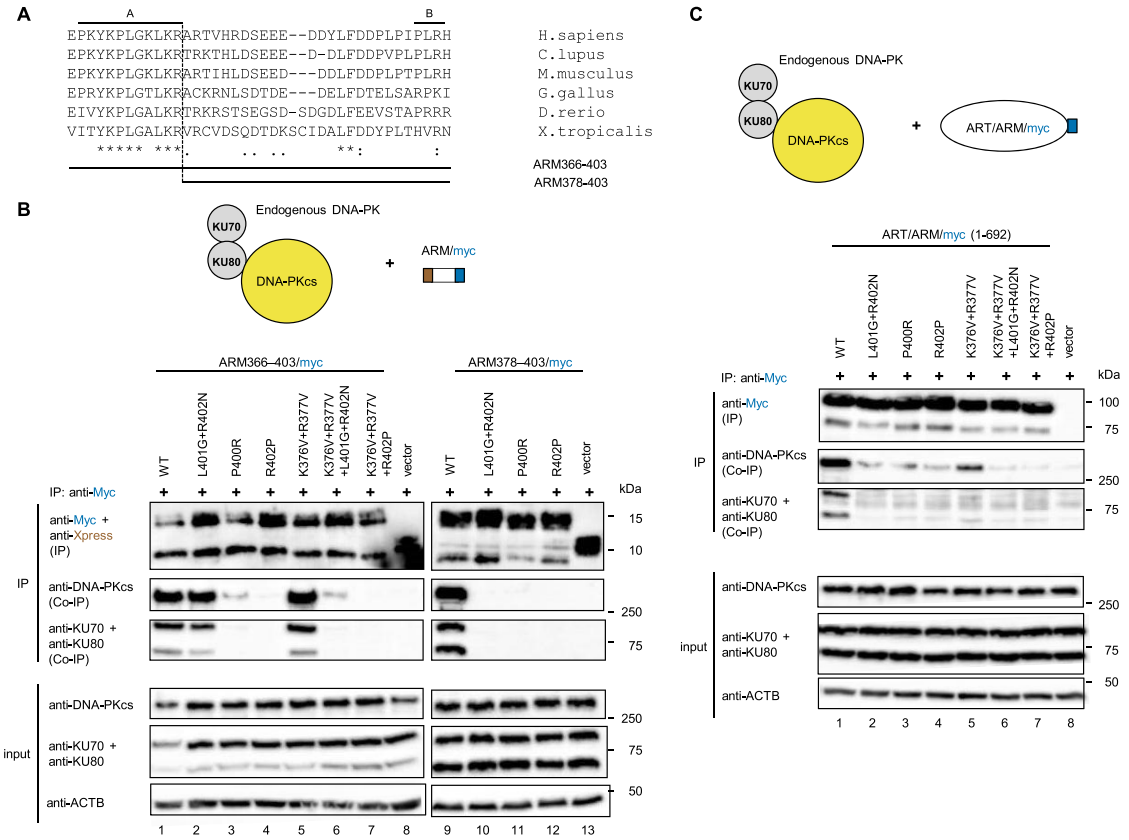

Figure 4. Definition of critical amino acids within the DNA-PKcs interaction domain of ARTEMIS. (**A**) Sequence alignment of ARTEMIS amino acids 366 to 403 in different species as specified. Below, horizontal lines indicate fragments ARM366-403 and ARM378-403. Asterisks, colons and periods indicate fully conserved, strongly and weakly similar residues, respectively (Clustal omega (61)). (B and C) HCT116 cells were transiently transfected with ARTEMIS-expressing plasmids containing either wildtype (WT) sequence or amino acid exchanges, as specified above each lane. The effect of each mutation was analysed in context of ARM366-403 and ARM378-403 (**B**) as well as in full-length ARTEMIS (1–692) (**C**). All ARTEMIS proteins have a C-terminal Myc-tag; ARTEMIS fragments in addition an N-terminal Xpress-tag. Interacting full-length proteins (circles and ellipses) and protein fragments (rectangles) are represented graphically at the top (not to scale). C-terminal Myc tags of the IP products are indicated as blue rectangles. Brown rectangles correspond to the N-terminal Max epitope. The Myc-tagged proteins were immunoprecipitated (IP) from cell lysates with anti-Myc antibody in buffer containing reduced detergent (0.01% NP40). This allowed detection of the DNA-PK holoenzyme as co-immunoprecipitate (Co-IP). Input and 80% of the IPs were separated in 8% SDS-PAGE and 20% of the IPs in 15% SDS-PAGE (B) or 8% SDS-PAGE (C), for detection of the IP products. Subsequently, western blotting was performed. Co-IP of endogenous DNA-PK was compared with input, using specific antibodies directed against DNA-PKcs, KU70 and KU80. IP products were identified using anti-Myc antibody, in case of ARM366-403 and ARM378-403 in combination with anti-Xpress antibody (B). The IP products of ARM366-403 and ARM378-403 appear as multiple bands, the nature of which is unclear. The theoretical molecular weights (MW) of the Xpress- and Myc-tagged ARTEMIS fragments are 11 kDa and 9.4 kDa for ARM366-403 and ARM378-403, respectively. The vector control results in an expressed fragment, containing in frame the Xpress- and Myc-tags, which together correspond to a theoretical MW of 7 kDa. The positions of protein standards are given at the right in kDa. Anti-β-actin (ACTB) antibody was used as loading control in input lanes. Two independent co-immunoprecipitation experiments were performed, and comparable results obtained.

affect the interaction of fragment PKcs3041-3082 (Figure 3B and C).

ARTEMIS amino acids 378–403 suffice for interaction with DNA-PKcs

Our next objective was to define a minimal fragment in ARTEMIS, capable of interaction with endogenous DNA-PKcs. Published results (18) indicate amino acid 403 in ARTEMIS as C-terminal border of the interaction domain (Supplementary Figure S2A). The experiments shown in Figure 3 identified amino acid 308 as possible N-terminal border of the DNA-PKcs interaction domain in ARTEMIS. There is a high degree of sequence conservation among species between amino acids 308 and 378 but only few conserved amino acids between 378 and 403 (Supplementary Figure S2B). We therefore constructed a set of N-terminal deletion mutants, each containing an N-terminal Xpress- and a C-terminal Myc-tag. All deletion mutants were of wildtype sequence or contained the double amino acid exchange L401G + R402N, which inhibits interaction between DNA-PKcs and full-length ARTEMIS (21). The ARTEMIS mutants were transiently expressed in HEK293T cells and co-immunoprecipitation experiments performed with buffer containing reduced NP40 concentration, allowing for detection of the association between ARTEMIS fragments and the endogenous DNA-PK holoenzyme (Supplementary Figure S2C). Surprisingly, deletion of the highly conserved region between amino acids 308 and 378 had no major effect on interaction with endogenous DNA-PK (Supplementary Figure S2C, lanes 1–15) but this is lost in ARM392-403 (Supplemen-

tary Figure S2C, lanes 15–19). In several deletion mutants amino acid exchanges L401G + R402N result in significantly higher IP product levels than in the wildtype counterparts (see lanes 3–10). Therefore in these cases, impairment of DNA-PK interaction might be underestimated. Interestingly, L401G + R402N impaired co-immunoprecipitation of DNA-PKcs in fragment ARM308-403, while in ARM366-403 significant residual activity is observed, which is lost in ARM378-403 (Supplementary Figure S2C, compare lanes 1, 2, 11–16). There is a region of high conservation between amino acids 366 and 378, which may be associated with these findings.

Next, we wanted to evaluate the effect of selected point mutations in conserved amino acids in the context of ARM366-403 and ARM378-403 (see Figure 4A). Experiments were performed in HCT116 cells, the results are depicted in Figure 4. There is some variation in expression levels of the ARTEMIS fragments, but in all cases immunoprecipitates of the mutant proteins are equivalent to or exceed wildtype levels (Figure 4B compare lanes 2–8 with lane 1 and lanes 10–12 with lane 9). Therefore, loss of co-immunoprecipitation of DNA-PK is not the result of reduced expression levels. In the context of ARM366-403 amino acid exchanges P400R and R402P drastically impaired interaction with DNA-PK (Figure 4B, lanes 3 and 4). Neither amino acid exchanges L401G + R402N nor K376V + R377V in the conserved region affected co-immunoprecipitation of DNA-PK significantly (Figure 4B, lanes 2 and 5). However, the combination of all four amino acid exchanges (K376V + R377V + L401G + R402N) impaired interaction with DNA-PK (Figure 4B, lane 6). In fragment ARM378-403, all mutations tested, also L401G + R402N, abolished interaction with DNA-PK (Figure 4B, lanes 10–13). Alanine substitutions confirmed the importance of amino acid positions P400 and R402 (Supplementary Figure S3).

The experimental results shown in Supplementary Figures S2, S4 and S3 establish that amino acids 378–403 in ARTEMIS are sufficient for DNA-PKcs interaction and the conserved amino acids 366–377 may contribute to binding activity. This is underscored by the observation that in ARM366-403 the combination of amino acid exchanges K376V + R377V + L401G + R402N abolishes interaction, while individually they have little impact on binding. Consistently, in the context of ARM378-403, L401G + R402N abolish interaction with DNA-PKcs. We therefore identified two critical regions within the DNA-PKcs interaction domain in ARTEMIS (regions A and B), which are illustrated as horizontal bars in Figure 4A.

The conserved region 366–378 is important for interaction between full-length ARTEMIS and endogenous DNA-PKcs

Having defined minimal DNA-PKcs-interacting ARTEMIS fragments and essential amino acids therein, next we wanted to analyse the same point mutations in full-length ARTEMIS. The results of the corresponding co-immunoprecipitation experiments in HCT116 cells are depicted in Figure 4C. Compared to wildtype protein, all mutations tested resulted in reduced DNA-PK interaction, with mutant R376V + R377V showing the most prominent residual binding activity (Figure 4C, lane 5). The combination of mutations in regions A and B, abolish interaction. Above we have shown that amino acid exchanges R376V + R377V and L402G + R402N individually had no effect on DNA-PKcs interaction with ARM366-403 (Figure 4B, lanes 2 and 5). In view of the differences in mutation sensitivity between full-length ARTEMIS and the DNA-PKcs interacting fragment ARM366-403, we wanted to verify, that in both cases, the interaction was DNA-independent. Supplementary Figure S4 documents, that both full-length ARTEMIS and ARM366-403 bind DNA-PKcs independently of DNA. The association between DNA-PKcs and the heterodimer KU70/KU80 is lost in the presence of ethidium bromide, in agreement with the need for the presence of DNA ends to build the DNA-PK holoenzyme. Compared to full-length ARTEMIS (ART-WT), ARM366-403 is expressed at significantly lower levels (see Supplementary Figure S4 detection of the IP product with anti-ARTEMIS antibody) however the amount of co-immunoprecipitated DNA-PK is increased. Therefore, Supplementary Figure S4 illustrates that the minimal ARTEMIS fragment binds endogenous DNA-PK much more strongly than full-length ARTEMIS (compare lanes 2 and 4 in Supplementary Figure S4).

ARTEMIS:DNA-PKcs interaction is necessary for V(D)J recombination

Up to now no experimental data exist, defining specific point mutations in ARTEMIS that impair DNA-PKcs interaction and *in vivo* V(D)J recombination. Having characterized the DNA-PKcs interaction domain in ARTEMIS in detail, we now wanted to evaluate the significance of the protein-protein interaction for ARTEMIS function. We established a *DCLRE1C*–/– knockout cell line derived from the HCT116 cell line used for the co-immunoprecipitation experiments. Using CRISPR/Cas9 technology, we introduced a homozygous deletion in the *DCLRE1C* gene, removing the promoter and exon 1. This strategy deletes the translational start site and amino acids up to position 45 contained in exon 1, resulting in a null mutation (19,42). We employed an extrachromosomal V(D)J recombination assay (17) to assess the functional importance of different amino acid exchanges in regions A and B of the DNA-PKcs interaction domain. To monitor differences in V(D)J recombination capability of ARTEMIS mutant proteins, it is important to use conditions in which ARTEMIS is the limiting factor. Therefore, V(D)J recombination activity was analysed for three different amounts of transfected ARTEMIS expression plasmids (150, 300 and 600 ng). In the case of ART-WT and mutant L401G + R402N in addition 75 ng were analysed, since in pilot experiments the expression of some mutant proteins was reduced 1.5–2-fold as compared to ART-WT and mutant L401G + R402N. For each sample, half of the harvested cells were analysed for V(D)J recombination activities and the other half was used to determine protein expression levels using anti-Myc antibody in western blot analyses (Supplementary Figure S5A-C). In addition, anti-ARTEMIS antibody was used to compare ART-WT/myc expression in HCT116 *DCLRE1C*–/– cells to the endogenous ARTEMIS protein levels in

HCT116 parental cells (Supplementary Figure S5D). Figure 5 summarizes the results of three independent V(D)J recombination experiments (Supplemental Table S1), the corresponding expression analyses are depicted in Supplementary Figure S5. The amino acid exchanges in regions A and B of the DNA-PKcs interaction domain in ARTEMIS mutant proteins (ARM) are specified below the columns. Mutations in either region A or B result in approximately 2-fold reduction in V(D)J recombination activity, while the combination of both decreases ARTEMIS function 5 to 10-fold. Transfection of 300 ng ART-WT/myc expression plasmid results in ARTEMIS protein close to the level of endogenous ARTEMIS in HCT116 parental cells (Supplementary Figure S5D).

The N-terminal nuclease domain by itself can mediate V(D)J recombination (19) and has DNA-PKcs-independent hairpin-opening activity in an *in vitro* nuclease assay (18). Region A of the DNA-PKcs interaction domain is close to the β-CASP domain in ARTEMIS, therefore we wanted to test the effect of amino acid exchanges K376V + R377V in the context of ARM1-383. Since the 7 N-terminal amino acids are essential for ARTEMIS function (19,42), we employed ARM8-382 as negative control. V(D)J recombination activities (Supplementary Figure S6A) and protein expression levels (Supplementary Figure S6C) were determined for each sample after transient transfections in HCT116 *DCLRE1C*–/– cells. While ARM8-383 has V(D)J recombination rates close to background level, ARM1-383 + K376V + R377V shows only a minor reduction in V(D)J recombination activity as compared to ARM1-383, if the differences in expression levels are considered.

DNA-PKcs interaction is necessary for V(D)J recombination independent of autoinhibitory self-interaction

Having established that mutations in the DNA-PKcs interaction domain affect V(D)J recombination activity we next wanted to investigate, whether this also holds true in the absence of ARTEMIS autoinhibitory self-interaction. We constructed an ARTEMIS mutant combining amino acid exchanges in the DNA-PKcs interaction domain (K376V + R377V + R402P) and in the autoinhibition domain (N456A + S457A + E458Q). Figure 6A shows a scheme of this ARTEMIS mutant and the relevant control proteins. All experiments were performed in HCT116 *DCLRE1C*–/– cells. First, we analysed the capability of the ARTEMIS proteins to co-immunoprecipitate endogenous DNA-PKcs. As expected, the triple point mutation K376V + R377V + R402P in the DNA-PKcs interaction domain in ARTEMIS impairs interaction with DNA-PKcs (Supplementary Figure S7, lanes 2 and 4). Expression of mutant C is reduced however co-immunoprecipitation of endogenous DNA-PKcs is comparable to ART-WT (compare IP and Co-IP signal intensities in lanes 1 and 3).

Co-immunoprecipitation by a C-terminal ARTEMIS fragment, capable of interaction with the ARTEMIS N-terminus, is evidence for loss of autoinhibitory self-interaction between the N- and C-termini of full-length ARTEMIS protein (19). In ART-WT and mutant A the N-termini are masked and not available for interaction with the isolated C-terminal fragment ARM414-692 (Figure 6B, lanes 1 and 2). Mutants B and C, both of which carry amino acid exchanges N456A + S457A + E458Q in the autoinhibitory domain, are readily co-immunoprecipitated by the C-terminal fragment (Figure 6B, lanes 3 and 4). As expected, the same mutations (N456A + S457A + E458Q) in the C-terminal fragment abolish these interactions (Figure 6B, lanes 5 and 6). Importantly, we can demonstrate interaction between the co-immunoprecipitated mutant B and endogenous DNA-PKcs. In the case of mutant C, the triple amino acid exchange in the DNA-PKcs interaction domain prevents this association (Figure 6B, compare lanes 3 and 4), underscoring the specificity of the observed interaction.

We performed V(D)J recombination experiments to address the question, whether physical interaction between ARTEMIS and DNA-PKcs is essential only for unmasking the N-terminal nuclease domain, or also for the subsequent hairpin-opening. Figure 6C summarizes the results of three independent V(D)J recombination experiments (Supplemental Table S2), the corresponding expression levels of the different ARTEMIS proteins are depicted in Supplementary Figure S8. In the context of mutations N456A + S457A + E458Q in the autoinhibitory domain (mutant B), additional amino acid exchanges in the DNA-PKcs interaction domain (mutant C) resulted in a significant decrease in V(D)J recombination activity. This finding indicates that DNA-PKcs interaction is important for ARTEMIS function also in ARTEMIS proteins, which have an unmasked N-terminus. Contrary to our previous results in ARTEMIS-deficient human dermal fibroblasts (19), mutations N456A + S457A + E458Q do not affect protein stability and we observe only a slight increase in V(D)J recombination activity of mutant B as compared to wildtype ARTEMIS.

DISCUSSION

The nuclease ARTEMIS and the protein kinase DNA-PKcs are factors of the NHEJ DNA repair pathway. While the association between both proteins has been described many years ago (7), there was a lack of experimental data showing the functional significance of this protein-protein interaction *in vivo*. Using co-immunoprecipitation experiments we characterized in detail the protein interaction domains in both proteins and tested the effect of specific amino acid exchanges in ARTEMIS on protein function in V(D)J recombination assays. The results of our protein interaction studies are summarized schematically in Supplemental Figure S9.

The ARTEMIS interaction domain in DNA-PKcs

Using co-immunoprecipitation experiments to monitor protein-protein interaction, in this study we show that mutation L3062R in DNA-PKcs substantially impairs its interaction with ARTEMIS (Supplementary Figure S9A). Previously, co-localisation of both wildtype and mutant DNA-PKcs with ARTEMIS at sites of DNA damage suggested that the interaction between ARTEMIS and DNA-PKcs was not affected by the pathogenic variant L3062R (29). While our biochemical experiments monitor physical inter-

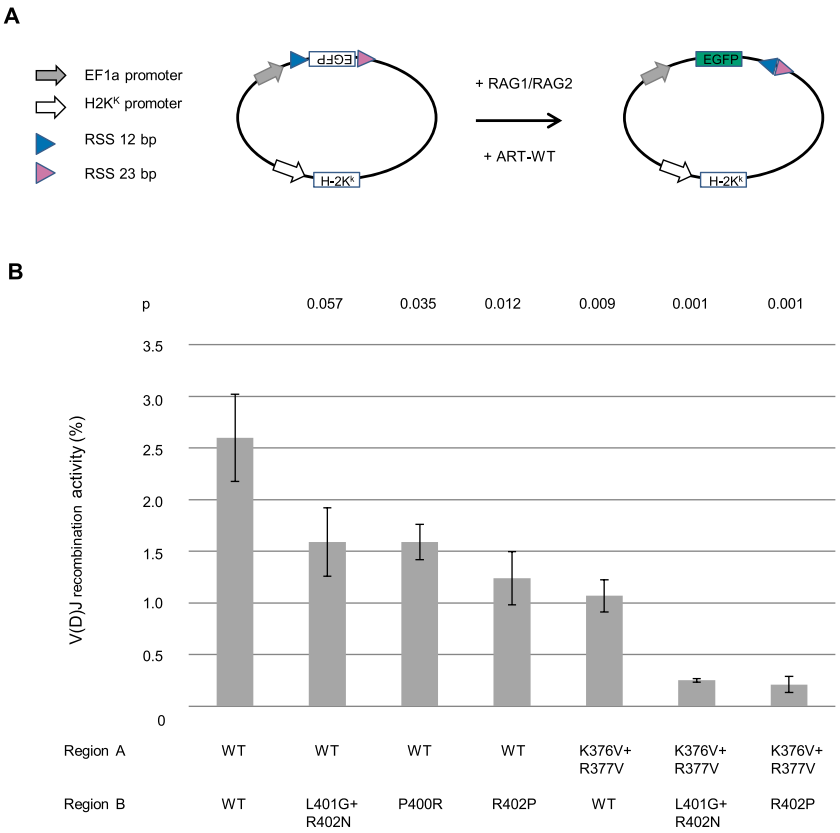

Figure 5. Amino acid exchanges in regions A and B of the DNA-PKcs interaction domain in ARTEMIS impair V(D)J recombination activity in HCT116 *DCLRE1C*–/– cells. HCT116 *DCLRE1C*–/– cells were co-transfected with V(D)J recombination substrate and plasmids expressing RAG1, RAG2 and Myc-tagged ARTEMIS proteins (wildtype or mutant). (**A**) Schematic of the V(D)J recombination substrate. Triangles indicate the Recombination Signal Sequences (RSS) surrounding the EGFP cDNA in antisense orientation. Arrows denote promoters driving expression of $H2K^K$ and EGFP. In the presence of transiently expressed RAG1, RAG2 and ARTEMIS proteins, the EGFP cassette is inverted, resulting in expression of EGFP protein. (**B**) V(D)J recombination activity was determined as the percentage of recombination-positive cells out of the subpopulation of transfected cells minus negative control (see Supplemental Table S1). V(D)J recombination activities at 150 ng ART-WT/ARM expression plasmids are shown as means of three independent experiments with standard deviations. P values for comparing ART-WT with each of the mutants were calculated using a two-tailed *t*-test and are given at the top. The amino acid exchanges in regions A and B of the DNA-PKcs interaction domain are specified below.

action between specific proteins, immunofluorescence studies describing co-localisation *in vivo* may not detect subtle changes in the interaction between individual proteins which are part of a multi-protein complex assembled at DSBs. Also, the fixing of cells prior to antibody staining may obscure changes in protein-protein interactions. Previously, van der Burg *et al.* have shown that V(D)J recombination activity is lost in CHO V3 cells, expressing human DNA-PKcs harbouring the patient variants. Together with our findings this suggests that loss of the direct ARTEMIS:DNA–PKcs interaction could be causative of the lack of ARTEMIS activation, resulting in a defect in V(D)J recombination and as a consequence a deficiency in the adaptive immune system. Interestingly, in other patients with amino acid exchange L3062R the clinical outcome shows immune dysregulation, resulting in autoimmunity, granuloma and late onset immunodeficiency (31,32).

With its 4128 amino acids DNA-PKcs is the biggest kinase in the PIKK family. We have identified a DNA-PKcs fragment of 42 amino acids (PKcs3041-3082) that binds ARTEMIS. However, in contrast to full-length DNA-PKcs, the amino acid exchange L3062R does not affect the interaction between PKcs3041-3082 and ARTEMIS (Figures 1 and 3, summarized in Supplemental Figure S9A and C). Our co-immunoprecipitation experiments indicate that PKcs3041-3082 binds ARTEMIS more strongly than full-length DNA-PKcs. Possibly a single amino acid exchange (L3062R) cannot disrupt this interaction. In this context, the conservation of the neighbouring L3061 may be indicative (Figure 2C). In L3062R an aliphatic side chain is changed to a positively charged one. This could induce intramolecular salt bridges affecting the tertiary structure of the full-length protein, but not the folding of the 42 amino acids in PKcs3041-3082. Additional regions in DNA-PKcs may also participate in the interaction with ARTEMIS. Intriguingly, in ARTEMIS we also identified specific amino acid exchanges (L401G + R402N, K376V + R377V) affecting the interaction between endogenous DNA-PKcs and the full-length protein (ART-WT, 1–692) but not with fragment ARM366-403.

To our knowledge, our results provide the first experimental data defining an ARTEMIS-interacting region in DNA-PKcs. The FAT region in DNA-PKcs is composed of

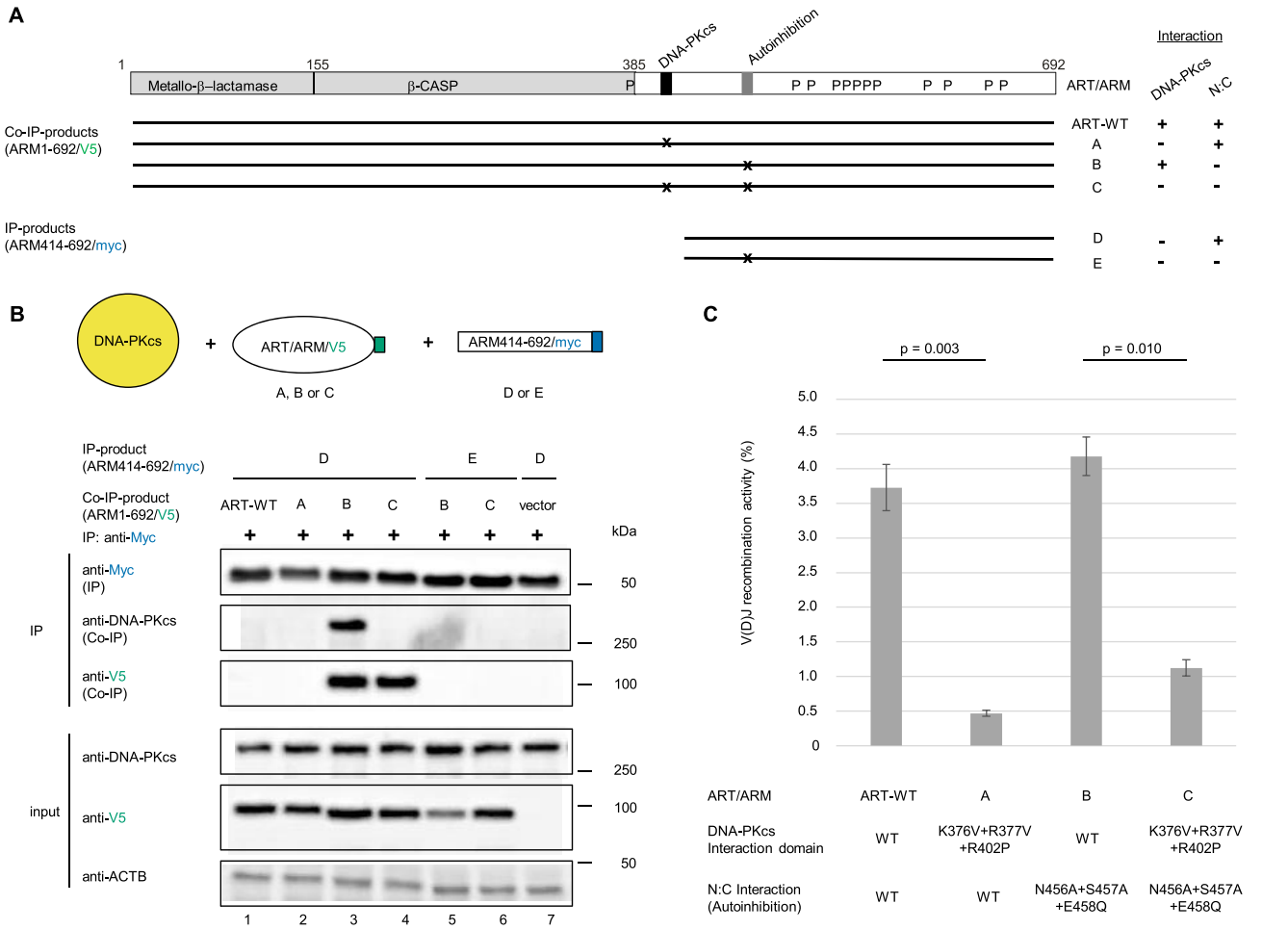

Figure 6. DNA-PKcs interaction is necessary for V(D)J recombination activities independent of autoinhibitory self-interaction. (**A**) Schematic of ARTEMIS indicating different protein domains (see Figure 3A for details). Below, full-length ARTEMIS proteins are represented as horizontal lines with x indicating mutations in the DNA-PKcs binding domain (K376V + R377V + R402P) and in the C-terminal autoinhibition domain (N456A + S457A + E458Q). On the right, DNA-PKcs and N:C self-interaction of ART-WT and mutants A–E are indicated by + and –, the results of the corresponding experiments are depicted in Figure 6B and Supplementary Figure S7. (**B**) Co-immunoprecipitation of full-length ARTEMIS proteins by the C-terminal ARTEMIS fragment ARM414-692, demonstrating loss of autoinhibitory self-interaction. HCT116 *DCLRE1C*–/– cells were transiently co-transfected with combinations of Myc-tagged ARM414-692 and V5-tagged full-length ARTEMIS, empty vector was used as negative control. The different interacting full-length proteins (circles and ellipses) and protein fragments (rectangles) are represented graphically at the top (not to scale). Immunological tags of IP (Myc) and Co-IP products (V5) are indicated in blue and green, respectively. Cell lysates were prepared and the Myc-tagged C-terminal fragments (ARM414-692) were immunoprecipitated (IP) with anti-Myc antibody. Western blotting was performed and co-immunoprecipitation (Co-IP) of V5-tagged full-length ARTEMIS (ART-WT/ARM) was compared to input using anti-V5 antibody. IP products were identified using anti-Myc antibody. Association of endogenous DNA-PKcs with the co-immunoprecipitated full-length ARTEMIS proteins was detected using anti-DNA-PKcs antibody. The positions of protein standards are given at the right in kDa. Anti-β-actin (ACTB) antibody was used as loading control in input lanes. Two independent co-immunoprecipitation experiments were performed, and comparable results obtained. (**C**) HCT116 *DCLRE1C*–/– cells were co-transfected with V(D)J recombination substrate (see Figure 5A), plasmids expressing RAG1, RAG2 and Myc-tagged full-length ARTEMIS of either wildtype sequence (WT) or containing mutations in the DNA-PKcs interaction domain or the C-terminal autoinhibitory domain as indicated below the columns. V(D)J recombination activity was determined as the percentage of recombination-positive cells out of the subpopulation of transfected cells minus negative control (see Supplemental Table S2). V(D)J recombination activities at 150 ng ART-WT/ARM expression plasmids are shown as means of three independent experiments with standard deviations. P values were calculated using a two-tailed *t*-test and are given at the top.

five supersecondary α-helical structures (FR1–FR5), which encircle the kinase domain (33,34). PKcs3041-3082 lies in FR2 and the cryo-EM analyses locate this region to the outside of the DNA-PKcs protein, supporting the idea of it being a protein interaction interface (33,34). PKcs3041-3082 is predicted to contain three α-helical motifs, with L3062 located in the middle helix (33). The sequence is highly conserved among species but is absent in the corresponding FAT regions in ATM and ATR (Figure 2). ARTEMIS is a phosphorylation target of ATM and together both proteins promote the repair of a subset of IR-induced DSB (35–38,43). Interactions between ARTEMIS and ATM and the MRN complex (Mre11, Rad50 and Nbs1) were described many years ago (37,38) however specific interaction domains have not been defined yet. We also show that the pathogenic variant L3062R in DNA-PKcs does not affect the interaction with the KU70/KU80 heterodimer. This agrees with the cryo-EM structures of DNA-PK, which identified KU interaction motifs in the HEAT repeats of DNA-PKcs (33,34,44).

The DNA-PKcs interaction domain in ARTEMIS

Previously, the analyses of C-terminal deletion mutants identified amino acids 398–403 in ARTEMIS as essential region for DNA-PKcs interaction (18). With a series of N-terminal deletion mutants, now we have defined ARM378-403 as a minimal DNA-PKcs interacting fragment. These results extend the observation that an *Escherichia coli* expressed ARTEMIS fragment encompassing amino acids 360–426 can bind purified DNA-PKcs (21). Our comparative analyses of ARTEMIS fragments and full-length proteins identified two regions of importance for DNA-PKcs interaction: conserved region A (aa 366–378), specified by amino acid exchanges K376V + R377V and region B, defined by mutation-sensitivity of the conserved amino acids P400 and R402. Region A is rich in positively charged residues and is predicted to adopt an α-helical structure, which is disrupted by amino acid exchanges K376V + R377V. This region is important for the interaction between DNA-PKcs and full-length ARTEMIS, but it is unimportant in ARM366-403 (Supplemental Figure S9B and E). Previously, we had shown that ARM1-383 cannot bind DNA-PKcs (18), indicating that region A alone is insufficient for DNA-PKcs interaction. Full-length DNA-PKcs and fragment PKcs3041-3082 co-immunoprecipitate the C-terminal half of ARTEMIS (ARM308-692) and both interactions depend on the presence of amino acids 308–347 (Supplemental Figure S9D). Strikingly, in the absence of the C-terminus, region 308–347 was dispensable for DNA-PKcs interaction. In summary, our data suggest that ARTEMIS amino acids 378–403 (region B) comprise the interaction interface and are necessary and sufficient for binding endogenous DNA-PKcs. In full-length ARTEMIS, region A (amino acids 366–377) and amino acids between positions 308 and 348 are necessary for the correct folding and positioning of the interaction interface. To date, no structural data of full-length ARTEMIS exist, but in the future the recently developed machine-learning modelling systems (45,46) may be valuable tools to verify the interpretation of our *in vitro* protein binding studies.

Our experiments define amino acids 366–403 as the DNA-PKcs interaction domain in ARTEMIS. Comparing input and Co-IP signals it is evident, that ARM366-403 has a much stronger binding activity than full-length ARTEMIS (Supplemental Figure S4). This observation could be related to the self-interaction between the ARTEMIS N- and C-termini, mediating autoinhibition in the full-length protein. The autoinhibitory domain is located approximately 50 amino acids C-terminal to the DNA-PKcs interaction domain, with amino acid exchanges at positions 454–458 abolishing self-interaction (19). N- and C-terminal deletion mutants removing either of the self-interaction domains, concomitantly result in increased co-immunoprecipitation efficacy (18) and this study. To a lesser degree, this is also the case for full-length ARM1-692 + N456A + S457A + E458Q, which has an open conformation. Using low detergent concentrations in our co-immunoprecipitation assays, we were able to show that ARTEMIS interacts with the DNA-PK holoenzyme. This holds true for the autoinhibited full-length ARTEMIS as well as for ARM366-403. Importantly, in both cases the interaction with DNA-PKcs is DNA-independent, while the association between DNA-PKcs and the KU70/80 heterodimer is DNA-dependent.

Specific amino acid exchanges in the DNA-PKcs interaction domain in ARTEMIS impair V(D)J recombination

Our experiments in the HCT116 *DCLRE1C*–/– knock out cell line establish that ARTEMIS:DNA-PKcs interaction is important for V(D)J recombination. Prerequisite for this finding was the detailed analyses of the DNA-PKcs interaction domain in ARTEMIS and V(D)J recombination assays performed at conditions where ARTEMIS is limiting. The combination of amino acid exchanges in regions A and B impairs V(D)J recombination. Mutations in either region reproducibly reduced V(D)J recombination rates about 2-fold, also in the case of mutants K376V + R378V and L401G + R402N. Interestingly, in our co-immunoprecipitation experiments with fragment ARM366-403, we observe similar results: Amino acid substitutions L401G + R402N and K376V + R378V alone had only a minor effect on DNA-PKcs interaction, whereas in combination interaction is lost (Supplemental Figure S9E). Previously, amino acid exchanges L401G + R402N in ARTEMIS were identified as critical for DNA-PKcs interaction, but no effect on V(D)J recombination in GUETEL-RSS cells was observed (21).

While the majority of pathogenic variants in ARTEMIS are deletions and amino acid exchanges in the N-terminal nuclease domain, only few variants have been described with small deletions in the C-terminal domain, resulting in truncated ARTEMIS proteins (27). No RS-SCID patient variant is known affecting amino acids located in the here defined DNA-PKcs interaction domain. This may be related to our finding, that loss of ARTEMIS function requires mutations in regions A and B of the interaction domain.

As discussed above, region 308–348 is important for interaction with DNA-PKcs. Because it is part of the ß-CASP domain and contains residues (e.g. H319), the mutation of which abolish nuclease activity (16,17), it was not possible to directly associate DNA-PKcs interaction with ARTEMIS function in V(D)J recombination assays. Conserved region A (aa 366–378) in ARTEMIS does not contain any core residues of the β-CASP domain (H165, H319 and V341) (13,16). Our experiments with C-terminally truncated ARTEMIS proteins show, that amino acid exchanges K376V + R377V only have a minor effect on ARTEMIS function. Recently, crystal structures of ARTEMIS catalytic core fragments have been published (47,48). ARTEMIS amino acids 1–361 were shown to be active in *in vitro* nuclease assays (48), indicating that region A is no essential part of the nuclease domain. Therefore, the drastic impairment of V(D)J recombination capability of ARM1-692 + K376V + R377V + R402P most likely is the result of loss of its DNA-PKcs interaction.

ARTEMIS:DNA-PKcs interaction is necessary for V(D)J recombination independent of autoinhibitory self-interaction

Self-interaction between the ARTEMIS C-terminus and the N-terminal nuclease domain mediate autoinhibition and DNA-PKcs dependent phosphorylation of the ARTEMIS

C-terminus was hypothesized to mediate relief of autoinhibition (20). However, mutation of 9 S/TQ phosphorylation sites in ARTEMIS did not affect V(D)J recombination and DSB repair (22) and phosphomimetic amino acid exchanges in the C-terminal domain did not induce an open conformation (19). In this study we investigated whether loss of DNA-PKcs interaction also affects ARTEMIS function, if the N-terminal nuclease domain in the full-length protein is unmasked. Indeed, in the context of amino acid exchanges N456A + S457A + E458Q, mutations in the DNA-PKcs interaction domain also reduce V(D)J recombination activity about 5-fold. In our co-immunoprecipitation experiments documenting the availability of the ARTEMIS N-terminus in mutant ARM1-692 + N456A + S457A + E458Q, we also observe its interaction with DNA-PKcs. Interestingly, compared to ART-WT, mutant ARM1-692 + N456A + S457A + E458Q exhibits increased binding of DNA-PKcs. Together these results suggest that ARTEMIS:DNA-PKcs interaction is necessary for V(D)J recombination independent of autoinhibitory self-interaction. Autophosphorylation of the ABCDE sites in DNA-PKcs is essential for ARTEMIS activation (22) and recently evidence has been put forward, that the presence of hairpins induces autophosphorylation at the ABCDE cluster, which leads to activation of ARTEMIS (24). The subsequent opening of the hairpins by the nuclease promotes additional DNA-PKcs autophosphorylation, as well as phosphorylation of other DNA-PK targets. Our data fit to this model of a stepwise activation process in V(D)J recombination and point to the need for a prolonged physical interaction between ARTEMIS and DNA-PKcs.

Recently, different experimental approaches have enhanced our understanding of the structure of and conformational changes in the NHEJ multiprotein complex. A long-range (LR) synaptic complex encompasses dimers of DNA-PK, Ligase 4, XRCC4 and XLF and protects the DNA ends. Autophosphorylation of DNA-PKcs induces the transition to the short-range (SR) complex, which is a prerequisite for end processing and subsequent ligation (49–52). In the SR complex DNA-PKcs has dissociated from DNA ends, but may still be in the vicinity, tethered by the C-terminal tail of KU80 (44). The ARTEMIS interaction site in DNA-PKcs defined by our biochemical experiments (PKcs3041-3082) is oriented to the outside of active and inactive DNA-PKcs, independent of the conformational changes in FR2 (53). To date no structural information for full-length ARTEMIS is available for evaluation of the localization of the DNA-PKcs interaction site in different stages of NHEJ. Our data suggest, that the interaction interface is accessible independent of autoinhibition and that interaction is necessary for V(D)J recombination. Single molecule imaging demonstrates that end-processing is restricted to the SR synaptic complex in which DNA-Ligase 4 regulates a hierarchical order of enzymes, maximizing the fidelity of DSB repair by NHEJ (50). Strikingly, depletion of ARTEMIS did not affect SR complex formation and processing of 5`flaps. In V(D)J recombination, error-prone end-processing is an important feature of B and T cell receptor diversity. Therefore, the regulation of the essential hairpin opening by DNA-PKcs activated ARTEMIS may differ from the repair of pathological DSB, 10% of which are ARTEMIS-dependent (35). For hairpin opening, ARTEMIS must be positioned close to the DNA ends, which are juxtaposed for ligation in the SR synaptic complex. ARTEMIS:DNA-PKcs interaction is DNA-independent, this may indicate that association occurs prior to SR complex formation. NHEJ is an iterative process (2) with a dynamic change between LR and SR synaptic complexes, mediated by DNA Ligase 4 (50). Interestingly, ARTEMIS also interacts with the ligase and the combination of mutations in the DNA-PKcs and DNA Ligase 4 interaction domains impair V(D)J recombination (54,55).

In summary, we provide evidence that the interaction between ARTEMIS and DNA-PKcs is necessary for V(D)J recombination, which is an essential step in lymphocyte development. In DNA-PKcs, pathogenic variant L3062R impairs interaction with ARTEMIS. In the case of ARTEMIS, we identified a combination of three amino acid exchanges which compromise both DNA-PKcs interaction and V(D)J recombination. Since both proteins are part of the NHEJ pathway, they are also involved in the repair of pathological DSB, as documented by the radiosensitivity of patient fibroblasts. The targeting of specific DNA repair pathways is considered a valuable tool in the treatment of drug-resistant tumours (56). Recently the association of the KU proteins with DNA has been exploited as target for the specific inhibition of DNA-PKcs kinase activity (57). The inhibition of a protein-protein interaction also can be conceived as a very specific tool in therapeutic targeting (58). Here, we have defined minimal protein-interacting fragments in DNA-PKcs and ARTEMIS, containing 42 and 25 amino acids, respectively. In the case of ARM378-403, the interaction with endogenous DNA-PKcs is much stronger compared to full-length ARTEMIS, making it a promising tool for inhibition of binding. Together with our finding that the ARTEMIS:DNA-PKcs interaction is a prerequisite for ARTEMIS function in the repair of physiological DSBs, this is a basis for the development of peptides and peptidomimetics to be used for the inhibition of DNA-PKcs-dependent ARTEMIS function in DNA repair.

While this work was under review elegant cryo-EM studies elucidated the structure of DNA-PK in association with full-length ARTEMIS and different DNA substrates (59). Intriguingly, L372 and L375 in ARTEMIS were shown to sandwich L3062 of DNA-PKcs and it was speculated that this hydrophobic cluster is important for ARTEMIS recruitment. Our biochemical and functional data characterizing in detail the ARTEMIS:DNA-PKcs interaction are in complete agreement with the results of the structural analyses. ARTEMIS residues L372 and L375 lie within conserved region A defined in our study as critical motif for both DNA-PKcs interaction and ARTEMIS function in V(D)J recombination. Mutation L3062R in DNA-PKcs abolishes interaction with ARTEMIS and leads to RS-SCID.

SUPPLEMENTARY DATA

Supplementary Data are available at NAR Online.

ACKNOWLEDGEMENTS

We are grateful to Ingrid Paper for excellent technical assistance, without which this work would not have been pos-

sible. We thank M. van der Burg, D. van Gent and D. Chen for the generous gift of CHO cell lines YFP/DNA–PKcs WT and mut, U. Pannicke for critical reading of the manuscript, J. Beck for providing plasmids PKcs2904-2945, PKcs3041-3082 and PKcs3041-3082 + L3062R, S. Radecke for the gift of Cas9 protein, E. Kuhn and N. Akgün for technical assistance.

Author contributions: D.N. and K.S. designed the study and analysed results. D.N. was responsible for experimental data and prepared the initial draft of the manuscript. Both authors contributed to the discussion and preparation of the final version of the manuscript.

FUNDING

Deutsche Forschungsgemeinschaft [SCHW 432/5-1 to K.S.]. Funding for open access charge: University of Ulm and Deutsche Forschungsgemeinschaft.

Conflict of interest statement. None declared.

REFERENCES

1. Lieber,M.R. (2010) The mechanism of double-strand DNA break repair by the nonhomologous DNA end-joining pathway. *Annu. Rev. Biochem.*, **79**, 181–211.
2. Pannunzio,N.R., Watanabe,G. and Lieber,M.R. (2018) Nonhomologous DNA end-joining for repair of DNA double-strand breaks. *J. Biol. Chem.*, **293**, 10512–10523.
3. Bassing,C.H., Swat,W. and Alt,F.W. (2002) The mechanism and regulation of chromosomal V(D)J recombination. *Cell*, **109**(Suppl), S45–S55.
4. Ochi,T., Wu,Q. and Blundell,T.L. (2014) The spatial organization of non-homologous end joining: from bridging to end joining. *DNA Repair*, **17**, 98–109.
5. Williams,G.J., Hammel,M., Radhakrishnan,S.K., Ramsden,D., Lees-Miller,S.P. and Tainer,J.A. (2014) Structural insights into NHEJ: building up an integrated picture of the dynamic DSB repair super complex, one component and interaction at a time. *DNA Repair*, **17**, 110–120.
6. Zhao,B., Rothenberg,E., Ramsden,D.A. and Lieber,M.R. (2020) The molecular basis and disease relevance of non-homologous DNA end joining. *Nat. Rev. Mol. Cell Biol.*, **21**, 765–781.
7. Ma,Y., Pannicke,U., Schwarz,K. and Lieber,M.R. (2002) Hairpin opening and overhang processing by an Artemis/DNA-dependent protein kinase complex in nonhomologous end joining and V(D)J recombination. *Cell*, **108**, 781–794.
8. Liang,S., Chaplin,A.K., Stavridi,A.K., Appleby,R., Hnizda,A. and Blundell,T.L. (2021) Stages, scaffolds and strings in the spatial organisation of non-homologous end joining: insights from X-ray diffraction and Cryo-EM. *Prog. Biophys. Mol. Biol.*, **163**, 60–73.
9. Imseng,S., Aylett,C.H. and Maier,T. (2018) Architecture and activation of phosphatidylinositol 3-kinase related kinases. *Curr. Opin. Struct. Biol.*, **49**, 177–189.
10. Gottlieb,T.M. and Jackson,S.P. (1993) The DNA-dependent protein kinase: requirement for DNA ends and association with ku antigen. *Cell*, **72**, 131–142.
11. Meek,K., Dang,V. and Lees-Miller,S.P. (2008) DNA-PK: the means to justify the ends?*Adv. Immunol.*, **99**, 33–58.
12. Davis,A.J., Chen,B.P.C. and Chen,D.J. (2014) DNA-PK: a dynamic enzyme in a versatile DSB repair pathway. *DNA Repair*, **17**, 21–29.
13. Callebaut,I., Moshous,D., Mornon,J.-P. and de Villartay,J.-P. (2002) Metallo-beta-lactamase fold within nucleic acids processing enzymes: the beta-CASP family. *Nucleic Acids Res.*, **30**, 3592–3601.
14. Ma,Y., Schwarz,K. and Lieber,M.R. (2005) The Artemis:DNA-pkcs endonuclease cleaves DNA loops, flaps, and gaps. *DNA Repair*, **4**, 845–851.
15. Chang,H.H.Y. and Lieber,M.R. (2016) Structure-Specific nuclease activities of artemis and the artemis:DNA-PKcs complex. *Nucleic Acids Res.*, **44**, 4991–4997.
16. Poinsignon,C., Moshous,D., Callebaut,I., de Chasseval,R., Villey,I. and de Villartay,J.-P. (2004) The metallo-beta-lactamase/beta-CASP domain of artemis constitutes the catalytic core for V(D)J recombination. *J. Exp. Med.*, **199**, 315–321.
17. Pannicke,U., Ma,Y., Hopfner,K.-P., Niewolik,D., Lieber,M.R. and Schwarz,K. (2004) Functional and biochemical dissection of the structure-specific nuclease ARTEMIS. *EMBO J.*, **23**, 1987–1997.
18. Niewolik,D., Pannicke,U., Lu,H., Ma,Y., Wang,L.-C.V., Kulesza,P., Zandi,E., Lieber,M.R. and Schwarz,K. (2006) DNA-PKcs dependence of artemis endonucleolytic activity, differences between hairpins and 5′ or 3′ overhangs. *J. Biol. Chem.*, **281**, 33900–33909.
19. Niewolik,D., Peter,I., Butscher,C. and Schwarz,K. (2017) Autoinhibition of the nuclease ARTEMIS is mediated by a physical interaction between its catalytic and C-terminal domains. *J. Biol. Chem.*, **292**, 3351–3365.
20. Ma,Y., Pannicke,U., Lu,H., Niewolik,D., Schwarz,K. and Lieber,M.R. (2005) The DNA-dependent protein kinase catalytic subunit phosphorylation sites in human artemis. *J. Biol. Chem.*, **280**, 33839–33846.
21. Soubeyrand,S., Pope,L., De Chasseval,R., Gosselin,D., Dong,F., de Villartay,J.-P. and Haché,R.J.G. (2006) Artemis phosphorylated by DNA-dependent protein kinase associates preferentially with discrete regions of chromatin. *J. Mol. Biol.*, **358**, 1200–1211.
22. Goodarzi,A.A., Yu,Y., Riballo,E., Douglas,P., Walker,S.A., Ye,R., Härer,C., Marchetti,C., Morrice,N., Jeggo,P.A. *et al.* (2006) DNA-PK autophosphorylation facilitates artemis endonuclease activity. *EMBO J.*, **25**, 3880–3889.
23. Douglas,P., Cui,X., Block,W.D., Yu,Y., Gupta,S., Ding,Q., Ye,R., Morrice,N., Lees-Miller,S.P. and Meek,K. (2007) The DNA-dependent protein kinase catalytic subunit is phosphorylated in vivo on threonine 3950, a highly conserved amino acid in the protein kinase domain. *Mol. Cell. Biol.*, **27**, 1581–1591.
24. Meek,K. (2020) Activation of DNA-PK by hairpinned DNA ends reveals a stepwise mechanism of kinase activation. *Nucleic Acids Res.*, **48**, 9098–9108.
25. Woodbine,L., Gennery,A.R. and Jeggo,P.A. (2014) The clinical impact of deficiency in DNA non-homologous end-joining. *DNA Repair*, **16**, 84–96.
26. Moshous,D., Callebaut,I., de Chasseval,R., Corneo,B., Cavazzana-Calvo,M., Le Deist,F., Tezcan,I., Sanal,O., Bertrand,Y., Philippe,N. *et al.* (2001) Artemis, a novel DNA double-strand break repair/V(D)J recombination protein, is mutated in human severe combined immune deficiency. *Cell*, **105**, 177–186.
27. Pannicke,U., Hönig,M., Schulze,I., Rohr,J., Heinz,G.A., Braun,S., Janz,I., Rump,E.-M., Seidel,M.G., Matthes-Martin,S. *et al.* (2010) The most frequent DCLRE1C (ARTEMIS) mutations are based on homologous recombination events. *Hum. Mutat.*, **31**, 197–207.
28. van der Burg,M., Verkaik,N.S., den Dekker,A.T., Barendregt,B.H., Pico-Knijnenburg,I., Tezcan,I., vanDongen,J.J.M. and van Gent,D.C. (2007) Defective artemis nuclease is characterized by coding joints with microhomology in long palindromic-nucleotide stretches. *Eur. J. Immunol.*, **37**, 3522–3528.
29. van der Burg,M., Ijspeert,H., Verkaik,N.S., Turul,T., Wiegant,W.W., Morotomi-Yano,K., Mari,P.-O., Tezcan,I., Chen,D.J., Zdzienicka,M.Z. *et al.* (2009) A DNA-PKcs mutation in a radiosensitive T-B- SCID patient inhibits artemis activation and nonhomologous end-joining. *J. Clin. Invest.*, **119**, 91–98.
30. Woodbine,L., Neal,J.A., Sasi,N.-K., Shimada,M., Deem,K., Coleman,H., Dobyns,W.B., Ogi,T., Meek,K., Davies,E.G. *et al.* (2013) PRKDC mutations in a SCID patient with profound neurological abnormalities. *J. Clin. Invest.*, **123**, 2969–2980.
31. Mathieu,A.-L., Verronese,E., Rice,G.I., Fouyssac,F., Bertrand,Y., Picard,C., Chansel,M., Walter,J.E., Notarangelo,L.D., Butte,M.J. *et al.* (2015) PRKDC mutations associated with immunodeficiency, granuloma, and autoimmune regulator-dependent autoimmunity. *J. Allergy Clin. Immunol.*, **135**, 1578–1588.
32. Esenboga,S., Akal,C., Karaatmaca,B., Erman,B., Dogan,S., Orhan,D., Boztug,K., Ayvaz,D. and Tezcan,İ. (2018) Two siblings with PRKDC defect who presented with cutaneous granulomas and review of the literature. *Clin. Immunol. Orlando Fla*, **197**, 1–5.
33. Sibanda,B.L., Chirgadze,D.Y., Ascher,D.B. and Blundell,T.L. (2017) DNA-PKcs structure suggests an allosteric mechanism modulating DNA double-strand break repair. *Science*, **355**, 520–524.

34. Yin,X., Liu,M., Tian,Y., Wang,J. and Xu,Y. (2017) Cryo-EM structure of human DNA-PK holoenzyme. *Cell Res.*, **27**, 1341–1350.
35. Riballo,E., Kühne,M., Rief,N., Doherty,A., Smith,G.C.M., Recio,M.-J., Reis,C., Dahm,K., Fricke,A., Krempler,A. *et al.* (2004) A pathway of double-strand break rejoining dependent upon ATM, artemis, and proteins locating to gamma-H2AX foci. *Mol. Cell*, **16**, 715–724.
36. Poinsignon,C., de Chasseval,R., Soubeyrand,S., Moshous,D., Fischer,A., Haché,R.J.G. and de Villartay,J.-P. (2004) Phosphorylation of artemis following irradiation-induced DNA damage. *Eur. J. Immunol.*, **34**, 3146–3155.
37. Zhang,X., Succi,J., Feng,Z., Prithivirajsingh,S., Story,M.D. and Legerski,R.J. (2004) Artemis is a phosphorylation target of ATM and ATR and is involved in the G2/M DNA damage checkpoint response. *Mol. Cell. Biol.*, **24**, 9207–9220.
38. Chen,L., Morio,T., Minegishi,Y., Nakada,S.-I., Nagasawa,M., Komatsu,K., Chessa,L., Villa,A., Lecis,D., Delia,D. *et al.* (2005) Ataxia-telangiectasia-mutated dependent phosphorylation of artemis in response to DNA damage. *Cancer Sci.*, **96**, 134–141.
39. Lees-Miller,J.P., Cobban,A., Katsonis,P., Bacolla,A., Tsutakawa,S.E., Hammel,M., Meek,K., Anderson,D.W., Lichtarge,O., Tainer,J.A. *et al.* (2021) Uncovering DNA-PKcs ancient phylogeny, unique sequence motifs and insights for human disease. *Prog. Biophys. Mol. Biol.*, **163**, 87–108.
40. Peterson,S.R., Kurimasa,A., Oshimura,M., Dynan,W.S., Bradbury,E.M. and Chen,D.J. (1995) Loss of the catalytic subunit of the DNA-dependent protein kinase in DNA double-strand-break-repair mutant mammalian cells. *Proc. Natl. Acad. Sci. U.S.A.*, **92**, 3171–3174.
41. Blunt,T., Finnie,N.J., Taccioli,G.E., Smith,G.C., Demengeot,J., Gottlieb,T.M., Mizuta,R., Varghese,A.J., Alt,F.W., Jeggo,P.A. *et al.* (1995) Defective DNA-dependent protein kinase activity is linked to V(D)J recombination and DNA repair defects associated with the murine scid mutation. *Cell*, **80**, 813–823.
42. Ege,M., Ma,Y., Manfras,B., Kalwak,K., Lu,H., Lieber,M.R., Schwarz,K. and Pannicke,U. (2005) Omenn syndrome due to ARTEMIS mutations. *Blood*, **105**, 4179–4186.
43. Beucher,A., Birraux,J., Tchouandong,L., Barton,O., Shibata,A., Conrad,S., Goodarzi,A.A., Krempler,A., Jeggo,P.A. and Löbrich,M. (2009) ATM and artemis promote homologous recombination of radiation-induced DNA double-strand breaks in g2. *EMBO J.*, **28**, 3413–3427.
44. Chaplin,A.K., Hardwick,S.W., Liang,S., Kefala Stavridi,A., Hnizda,A., Cooper,L.R., De Oliveira,T.M., Chirgadze,D.Y. and Blundell,T.L. (2021) Dimers of DNA-PK create a stage for DNA double-strand break repair. *Nat. Struct. Mol. Biol.*, **28**, 13–19.
45. Baek,M., DiMaio,F., Anishchenko,I., Dauparas,J., Ovchinnikov,S., Lee,G.R., Wang,J., Cong,Q., Kinch,L.N., Schaeffer,R.D. *et al.* (2021) Accurate prediction of protein structures and interactions using a three-track neural network. *Science*, **373**, 871–876.
46. Jumper,J., Evans,R., Pritzel,A., Green,T., Figurnov,M., Ronneberger,O., Tunyasuvunakool,K., Bates,R., Žídek,A., Potapenko,A. *et al.* (2021) Highly accurate protein structure prediction with alphafold. *Nature*, **596**, 583–589.
47. Karim,M.F., Liu,S., Laciak,A.R., Volk,L., Koszelak-Rosenblum,M., Lieber,M.R., Wu,M., Curtis,R., Huang,N.N., Carr,G. *et al.* (2020) Structural analysis of the catalytic domain of artemis endonuclease/SNM1C reveals distinct structural features. *J. Biol. Chem.*, **295**, 12368–12377.
48. Yosaatmadja,Y., Baddock,H.T., Newman,J.A., Bielinski,M., Gavard,A.E., Mukhopadhyay,S.M.M., Dannerfjord,A.A., Schofield,C.J., McHugh,P.J. and Gileadi,O. (2021) Structural and mechanistic insights into the artemis endonuclease and strategies for its inhibition. *Nucleic Acids Res.*, **49**, 9310–9326.
49. Graham,T.G.W., Walter,J.C. and Loparo,J.J. (2016) Two-stage synapsis of DNA ends during non-homologous end joining. *Mol. Cell*, **61**, 850–858.
50. Stinson,B.M., Moreno,A.T., Walter,J.C. and Loparo,J.J. (2020) A mechanism to minimize errors during Non-homologous end joining. *Mol. Cell*, **77**, 1080–1091.
51. Chen,S., Lee,L., Naila,T., Fishbain,S., Wang,A., Tomkinson,A.E., Lees-Miller,S.P. and He,Y. (2021) Structural basis of long-range to short-range synaptic transition in NHEJ. *Nature*, **593**, 294–298.
52. Chaplin,A.K., Hardwick,S.W., Stavridi,A.K., Buehl,C.J., Goff,N.J., Ropars,V., Liang,S., De Oliveira,T.M., Chirgadze,D.Y., Meek,K. *et al.* (2021) Cryo-EM of NHEJ supercomplexes provides insights into DNA repair. *Mol. Cell*, **81** , 3400–3409.
53. Chen,X., Xu,X., Chen,Y., Cheung,J.C., Wang,H., Jiang,J., de Val,N., Fox,T., Gellert,M. and Yang,W. (2021) Structure of an activated DNA-PK and its implications for NHEJ. *Mol. Cell*, **81**, 801–810.
54. Malu,S., De Ioannes,P., Kozlov,M., Greene,M., Francis,D., Hanna,M., Pena,J., Escalante,C.R., Kurosawa,A., Erdjument-Bromage,H. *et al.* (2012) Artemis C-terminal region facilitates V(D)J recombination through its interactions with DNA ligase IV and DNA–PKcs. *J. Exp. Med.*, **209**, 955–963.
55. De Ioannes,P., Malu,S., Cortes,P. and Aggarwal,A.K. (2012) Structural basis of DNA ligase IV-Artemis interaction in non-homologous end joining (NHEJ). *Cell Rep.*, **2**, 1505–1512.
56. Huang,R.-X. and Zhou,P.-K. (2020) DNA damage response signaling pathways and targets for radiotherapy sensitization in cancer. *Signal Transduct. Target. Ther.*, **5**, 60.
57. Gavande,N.S., VanderVere-Carozza,P.S., Pawelczak,K.S., Mendoza-Munoz,P., Vernon,T.L., Hanakahi,L.A., Summerlin,M., Dynlacht,J.R., Farmer,A.H., Sears,C.R. *et al.* (2020) Discovery and development of novel DNA-PK inhibitors by targeting the unique Ku-DNA interaction. *Nucleic Acids Res.*, **48**, 11536–11550.
58. Corbi-Verge,C. and Kim,P.M. (2016) Motif mediated protein-protein interactions as drug targets. *Cell Commun. Signal. CCS*, **14**, 8.
59. Liu,L., Chen,X., Li,J., Wang,H., Buehl,C.J., Goff,N.J., Meek,K., Yang,W. and Gellert,M. (2022) Autophosphorylation transforms DNA-PK from protecting to processing DNA ends. *Mol. Cell*, **82**, 177–189.
60. Lu,S., Wang,J., Chitsaz,F., Derbyshire,M.K., Geer,R.C., Gonzales,N.R., Gwadz,M., Hurwitz,D.I., Marchler,G.H., Song,J.S. *et al.* (2020) CDD/SPARCLE: the conserved domain database in 2020. *Nucleic Acids Res.*, **48**, D265–D268.
61. Madeira,F., Park,Y.M., Lee,J., Buso,N., Gur,T., Madhusoodanan,N., Basutkar,P., Tivey,A.R.N., Potter,S.C., Finn,R.D. *et al.* (2019) The EMBL-EBI search and sequence analysis tools APIs in 2019. *Nucleic Acids Res.*, **47**, W636–W641.